Research Article

Nanopumping Molecules via a Carbon Nanotube

Min Chen[1,2,3], Ji Zang[3], Dingquan Xiao[1], C. Zhang[4], and Feng Liu[3] （✉）

[1] Department of Materials Science and Engineering, Sichuan University, Chengdu, Sichuan 610064, China

[2] Department of Optoelectronic Technology, Chengdu University of Information Technology, Chengdu, Sichuan 610225, China

[3] Department of Materials Science and Engineering, University of Utah, Salt Lake City, Utah 84112, USA

[4] School of Engineering Physics, University of Wollongong, New South Wales 2522, Australia

ABSTRACT

We demonstrate the feasibility of using a carbon nanotube to nanopump molecules. Molecular dynamics simulations show that the transport and ejection of a C_{20} molecule via a single-walled carbon nanotube (SWNT) can be achieved by a sustained mechanical actuation driven by two oscillating tips. The optimal condition for nanopumping is found when the tip oscillation frequency and magnitude correlate to form quasi steady-state mechanical wave propagation in the SWNT, so that the energy transfer process is optimal leading to maximal molecular translational motion and minimal rotational motion. Our finding provides a potentially useful mechanism for using an SWNT as a vehicle to deliver large drug molecules.

KEYWORDS

Introduction

Some important applications of carbon nanotubes (CNTs) lie in the area of biomedical science and biotechnology [1]. For example, CNTs have been proposed as a nanoscale vehicle for drug delivery [1–3] and formed the basis of the development of a new *in situ* human organ pressure monitor [4–5]. A CNT is small enough to cross the cell membrane in a harmless manner and enter the nucleus of the cell, while the cell does not recognize the nanotube as an unfriendly intruder [6]. Therefore, a CNT can be used effectively as a vehicle to deliver drugs to the targeted sick cell (such as a cancer cell) with unprecedented accuracy and efficiency. One possible way to direct the motion of CNTs for drug delivery is CNT spearing, based on the penetration of nickel-embedded CNTs into cell membranes driven by a magnetic field [7].

To fulfill the drug delivery process, drug molecules may be attached to a CNT and then released after being carried by the CNT to the targeted areas. A number of studies have demonstrated the feasibility of attaching molecules to a CNT via surface functionalization [2, 8, 9]. Drug molecules may also be placed inside a CNT for delivery. Molecular dynamics (MD) simulations showed that a DNA molecule could be spontaneously encapsulated into a CNT in aqueous solution [10]. Furthermore, transporting and nanopumping atoms

Address correspondence to fliu@eng.utah.edu

and molecules inside a CNT have been shown using a variety of different actuation mechanisms, driven by thermal [11], electrical [3, 12], optical [13], or mechanical [14, 15] effects.

Because of the attractive interactions, such as van der Waals attraction, between a guest molecule and a CNT, the molecule would prefer to stay inside the CNT in the ground state [10]. In general, there is an energy barrier preventing an encapsulated molecule inside a CNT from coming out of the CNT [16]. Therefore, one needs to search for an effective actuation mechanism to eject the molecule out of the single-walled carbon nanotube (SWNT) for drug delivery. An interesting domino process in SWNTs was recently proposed by Chang [17]. However, such a domino process is only applicable to large tubes when their ground state has a collapsed shape and the circular tube is metastable. Here, we propose a different actuation mechanism via mechanical wave propagation, which is applicable to small tubes. So, these two methods are complementary to each other working with different driving mechanisms and in different ranges of tube diameters. We point out that practically, our proposal of working with small tubes may have two advantages. First, most synthesis methods produce SWNTs of small diameters while larger ones are less common. Second, large SWNTs often take the ground-state collapsed shape [18] rather than the metastable circular shape, preempting use of the domino process.

Specifically, we propose to actuate mechanical wave propagation in an SWNT by two oscillating tips [19]. Using MD simulations that include the tip effect, we demonstrate mechanical nanopumping of a C_{20} molecule via an SWNT. Two tips placed in one end of the SWNT oscillate in such a way as to generate sustained propagating mechanical waves in the tube, which drive and accelerate the molecule inside until ejecting it out from the other end of the tube. We investigate the optimal tip oscillation conditions (i.e., the oscillation frequency and magnitude) in order to find the highest nanopumping efficiency that produces the largest molecule acceleration and ejection speed.

Our MD simulation setup and procedure are shown in Fig. 1(a). A C_{20} molecule encapsulated inside a (13, 0) SWNT was chosen as a model system, and was shown to be a stable system based on their respective sizes [16, 20]. Two tips are placed at one end of the tube, which oscillate as a mechanical actuator to generate mechanical wave propagation in the tube as studied previously for the free tubes without the encapsulated molecule [19]. The carbon–carbon interactions in the (13, 0) SWNT and C_{20} molecule were described by the Tersoff bond-order [21] potential, and the C_{20}–tube interaction was described by a Lennard-Jones potential [22]. We used the Hoover thermostat to perform the MD simulations in the (N,V,T) ensemble at 300 K and a 5th order predictor–corrector algorithm to integrate the equation of motion. The time step was set at 0.2 fs with a total simulation time of up to 20 ps. The system was first brought into equilibrium at 300 K, before applying the tip actuation for the nanopumping process.

The static energy barrier for a C_{20} molecule to come out from a (13, 0) SWNT is calculated to be 1.48 eV. Therefore, the C_{20} has to be accelerated inside the (13, 0) tube to gain sufficient kinetic energy to overcome this barrier, in order to realize the
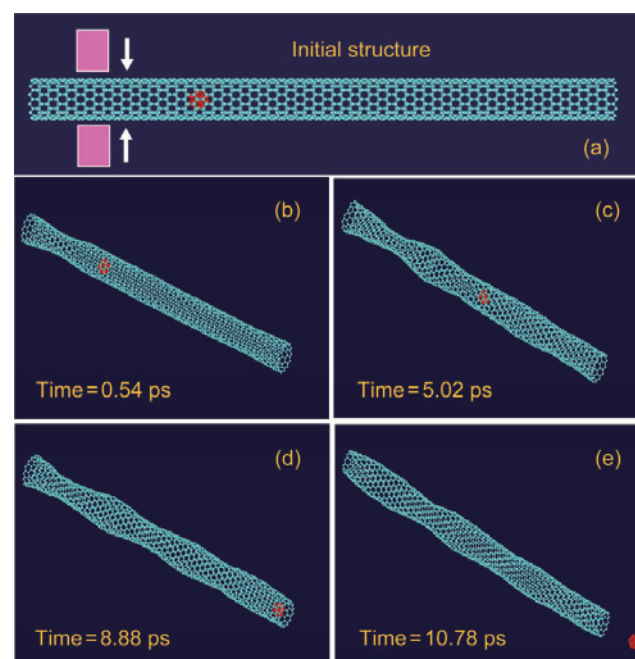

Figure 1 (a) Illustration of simulation setup for nanopumping. (b) to (e) Snapshots of a successful nanopumping process of C_{20} via a (13, 0) SWNT. Tip oscillation magnitude is 2.083 Å. Tip oscillation frequency is 1 THz. Tube length is 136 Å

nanopumping process. Our previous studies showed that sustainable mechanical wave propagation can be generated by a two-tip actuator [19]. For a (13, 0) tube, the mechanical wave velocity can reach as high as 5000 m/s. Now, in the presence of a C_{20} molecule, as the tip-actuated mechanical wave meets the molecule, the locally deformed (compressed) tube wall will repel the C_{20} driving (squeezing) it to move along the wave propagation direction. The idea is to find optimal tip actuation conditions that will lead to successful nanopumping (accelerating and ejecting) of the C_{20} molecule by the (13, 0) SWNT.

Figures 1(b)–(e) show an example of the simulation of a successful nanopumping process. The details of the whole process can be viewed online in the video in the Electronic Supplementary Material (ESM). At the beginning, the C_{20} is loaded inside next to the two tips placed at one end of the (13, 0) tube. As the tips oscillate, the tip-actuated mechanical wave starts to drive the C_{20} to move towards the right due to the repulsive force between the molecule and the deformed tube (Fig. 1(b)). The mechanical waves are generated gradually and sustained throughout the simulation, and accelerate the molecule causing it to move continuously in the direction of the mechanical wave propagation (Fig. 1(c)). After ~9 ps, the C_{20} approaches the other free end of the tube (Fig. 1(d)); at ~10 ps, the C_{20} is finally ejected out of the tube (Fig. 1(e)), completing the nanopumping process.

The nanopumping process consists of two key steps of transporting (i.e., accelerating) the molecule inside the tube and ejecting the molecule out of the tube. These can be analyzed by examining the molecule axial velocity as a function of time and tip position as shown in Fig. 2. It is found that most acceleration of C_{20} occurs in the first 2.0 ps over a short distance of ~6–7 Å (Fig. 2), during which the axial velocity of C_{20} increases from 0 to ~1100 m/s corresponding to a very large acceleration of ~5.5×10^{14} m/s². Then, the C_{20} continues to accelerate at a slower rate for the next 2.5 ps over a distance of ~25 Å reaching the maximum axial velocity of 1500 m/s at an average acceleration of ~1.6×10^{14} m/s². After that the C_{20} gradually slows down, decelerating uniformly to an axial velocity of ~1000 m/s upon reaching the

right-hand open end of the tube before being ejected out of the tube. During the ejection process, as seen at the end of the tube (marked with a vertical dashed line in Fig. 2), the C_{20} velocity first increases slightly as it comes out of the tube but remains bonded with the tube atoms at the end, and then decreases rapidly after breaking the bonds with the tube atoms to become free.

Despite the slow-down of C_{20} as it reaches the right-hand end of the tube, it still possesses sufficient kinetic energy to overcome the potential energy barrier to moving out of the tube. The ejection speed, i.e., the instantaneous axial velocity of C_{20} leaving the right-hand end of the tube is ~1200 m/s. As soon as the molecule is ejected out from the tube, its axial velocity decreases rapidly in the vacuum. MD simulations showed that in addition to the lateral translational motion driven by the mechanical wave, the encapsulated C_{20} also has a rotational motion, i.e., it simultaneously rotates as it translates from left to right. So, through the interaction between C_{20} and the tube wall, the tube mechanical wave transfers the energy into the C_{20} in two kinetic energy forms of translational motion and rotational motion. The fluctuation of C_{20} axial velocity, i.e., translational kinetic energy, as shown in Fig. 2, is largely caused by exchange of these two forms of kinetic energy.
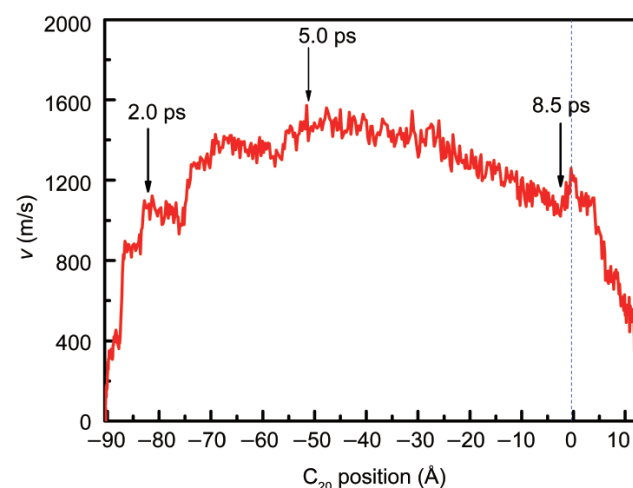

Figure 2   Axial velocity of C_{20} as a function of its position inside the tube during the nanopumping process corresponding to Fig. 1. The right-hand end of the tube is set to be the position zero (vertical dashed line). The three arrows mark the time at different positions, indicating three stages of acceleration and deceleration of C_{20} inside the tube

When the molecule rotates rapidly, it will slow down its translational motion along the tube axis. Thus, it is desirable to minimize the rotational motion in order to increase nanopumping efficiency. The rotational motion of C_{20} is possibly caused by its spherical shape giving a small momentum of inertia for rotation. We expect that a non-spherical molecule would undergo less rotation.

A focus of our study is to investigate the efficiency of nanopumping driven by wave propagation and thus find the optimal tip actuation conditions for nanopumping. Most importantly, we found that not all the nanopumping processes are successful and the efficiency of nanopumping depends strongly on the form of mechanical waves generated by the tip actuator, which in turn depends on the tip oscillation conditions. The encapsulated C_{20} can be pumped out of the (13, 0) tube when the two tips oscillate with a correlation between the tip oscillation frequency and magnitude that generates a sustainable traveling wave corresponding to the similar condition for generating the quasi steady-state standing waves in a free (13, 0) nanotube without molecule encapsulation [19].

For a given tube length, it has been shown that a smaller tip oscillation magnitude combined with a higher tip oscillation frequency can sustain a more steady mechanical wave in free SWNTs [19]. This indicates that a more stable mechanical wave is desirable for accelerating the molecule inside the tube. Moreover, MD simulations showed that the barrier at the right-hand end of the tube is dynamically changed in the presence of a mechanical wave and is different from the original theoretical barrier for a stationary tube, and furthermore it is slightly different for different waves in every nanopumping process. Therefore, the overall nanopumping process is decided by the optimization of tip actuations to generate a stable sustainable mechanical wave that will both accelerate the molecule inside the tube for transportation and overcome the dynamic barrier at the end of tube for ejecting the molecule.

When the tip actuator does not oscillate according to the desired correlated conditions, our simulations show that the nanopumping process may fail to eject the C_{20} molecule from (13, 0) SWNT, as shown in Fig. 3. This is because away from the optimal tip oscillation magnitude or frequency, the tip actuation cannot generate a steady mechanical wave, but instead the wave dies out with time, as in a free tube [19]. Furthermore, a non-steady irregular wave tends to induce large rotation of C_{20} causing the whole tube to bend at the same time (Fig. 3). These actions all dissipate a lot of energy and reduce the acceleration of C_{20} in the axial direction. Whenever these two effects are significant, the nanopumping process fails.

We can examine the effectiveness of nanopumping process by analyzing the energy transfer process in terms of kinetic energy partition between the translational and rotational motion. Figure 4 shows a comparison of the kinetic energy partition between a successful and a failed nanopumping process. In a successful nanopumping process (Fig. 4(a)), the tube mechanical wave energy is transferred into the C_{20} mostly in the form of translational kinetic energy, while the gain in rotational kinetic energy is very small. Consequently, the C_{20} gains up to ~2 eV of translational kinetic energy in the first few ps
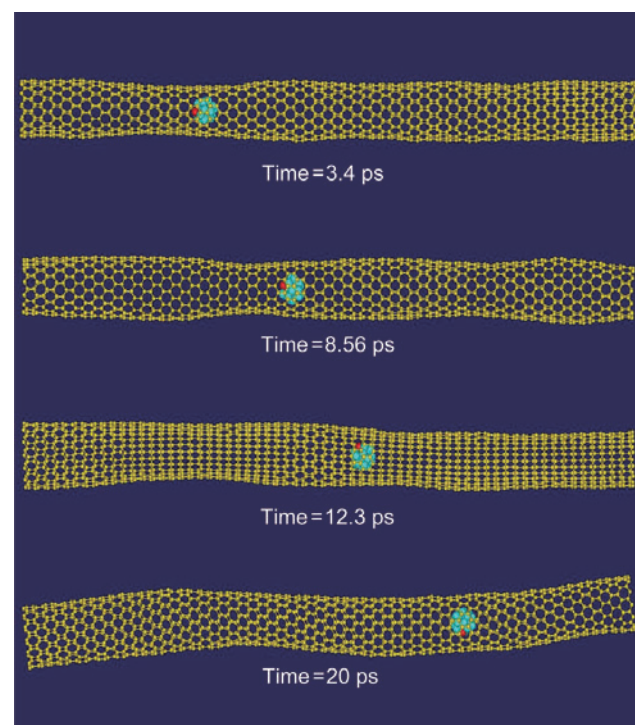

Figure 3 Snapshots of a failed nanopumping process of C_{20} via a (13, 0) SWNT. One atom in C_{20} is marked red to show the rotational motion of C_{20}. Tip oscillation magnitude is 1.583 Å. Tip oscillation frequency is 0.25 THz. Tube length is 136 Å

and is then ejected out at ~9.8 ps. In contrast, in a failed nanopumping process (Fig. 4(b)), a significant fraction of the tube mechanical wave energy is transferred into the C_{20} rotational kinetic energy. Consequently, the C_{20} gains much less translational kinetic energy (less than ~0.45 eV), which is not enough for ejection of the molecule out of the tube even after 20 ps of simulation.

Because successful nanopumping can only be achieved with certain correlated tip oscillation magnitudes and frequencies, we have carried out extensive MD simulations to determine the suitable range of the tip oscillation magnitudes and frequencies leading to successful nanopumping, and constructed a phase diagram as shown in Fig. 5. It is found that the range of tip oscillation magnitudes for successful nanopumping is from 0.583 to 3.583 Å using (13, 0) SWNT. If the tip oscillation magnitude is too small (<0.583 Å), the mechanical wave does not generate enough force and energy to drive the molecule. If the tip oscillation magnitude is too large (>3.583 Å), it causes the upper portion of the tube to form bonds with the lower part in the compressed regions between the two tips leading to breakdown of actuation.

At any given tip oscillation magnitude between 0.583 Å and 3.583 Å, the desired tip frequency for successful nanopumping is different. In general, a larger oscillation magnitude requires lower frequencies. For example, when the tip oscillation magnitude is 3.083 Å, the range of successful tip frequencies is 0.15–0.71 THz, as shown in Fig. 5. If the frequency is lower than 0.15 THz, C_{20} exhibits large rotational motion and the tube begins to bend. Consequently, the C_{20} will either fail to reach the other end of the tube, or fail to come out of the tube even if it reaches the end of the tube. If the frequency is higher than 0.71 THz, no obvious mechanical wave can be generated in the tube, due to the lack of time for the tube to respond to the tip oscillation.

Different forms of mechanical wave in (13, 0) SWNT drive the encapsulated C_{20} molecule with different efficiencies. In particular, the acceleration of the C_{20} molecule inside the tube increases with the increasing tip frequency, but it can decrease if the frequency is too high. The reason is that the higher
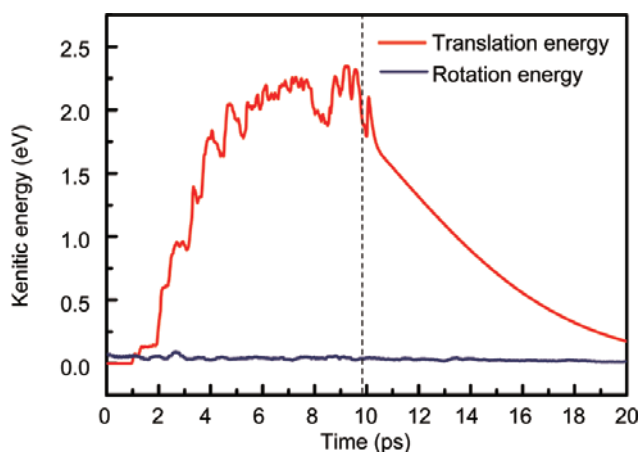
(a)
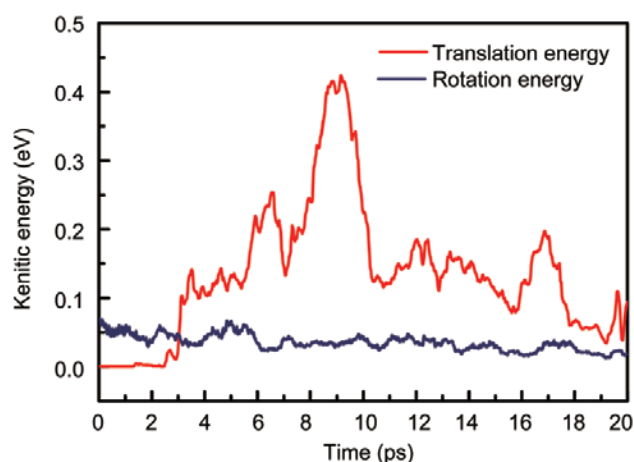
(b)

Figure 4 Comparison of kinetic energy partition between the translational and rotational motion of C_{20} in (a) a successful pumping process versus in (b) a failed pumping process
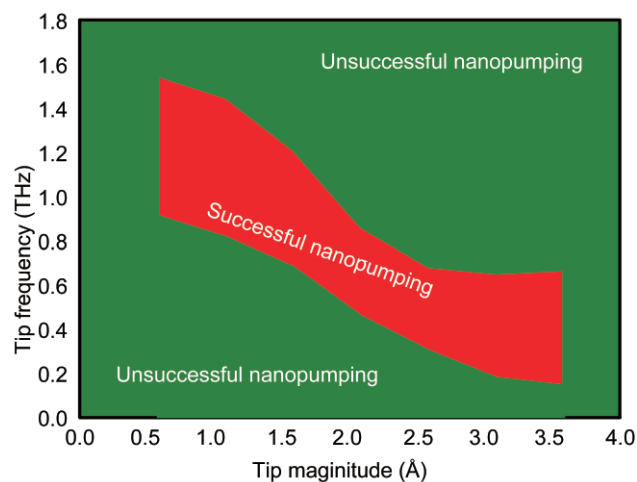

Figure 5 Phase diagram that defines the range of tip oscillation magnitudes and frequencies for successful nanopumping

driving tip frequency has a higher "horsepower" injecting more energy per unit time into the tube. But, if the frequency is too high, the tube cannot mechanically respond to the tip oscillation. On the other hand, for the successful nanopumping processes, the molecule ejection velocities are quite different under different tip conditions (see Table S-1 in the ESM where a few examples of different accelerations and ejection speeds of C_{20} resulting from different tip oscillation magnitudes and frequencies are listed). This is because the energy transfer process between the molecule and the SWNT varies for different mechanical waves generated in the tube, leading to different molecular transport processes and ejection behaviors. The maximum acceleration and ejection velocities of C_{20} via a (13, 0) SWNT we achieved are 3.44×10^{14} m/s^2 and 2176 m/s, respectively.

In summary, using MD simulations we have demonstrated the feasibility of using SWNTs for nanopumping molecules via mechanical wave propagation driven by an oscillating tip actuator. We found that there exists an optimal tip oscillation condition for the nanopumping process, which corresponds to the generation of quasi steady-state wave propagation in the tube so that the tube mechanical wave energy is transferred mostly to the molecular translational motion rather than the rotational motion. The nanopumping is usually more efficient using smaller tip oscillation magnitudes and higher frequencies. Our proposed nanopumping process using small tubes is complementary to the domino process using large tubes [17]. These findings may help develop a useful approach for drug delivery using SWNTs.

Acknowledgements

References

[1] Martin, C. R.; Kohli, P. The emerging field of nanotube biotechnology. *Nat. Rev. Drug Discov.* **2003**, *2,* 29–37.

[2] Kam, N. W. S.; Dai, H. J. Carbon nanotubes as intracellular protein transporters: Generality and biological functionality. *J. Am. Chem. Soc.* **2005**, *127,* 6021–6026.

[3] Svensson, K.; Olin, H.; Olsson, E. Nanopipettes for metal transport. *Phys. Rev. Lett.* **2004**, *93,* 145901.

[4] Wu, J.; Zang, J.; Larade, B.; Guo, H.; Gong, X. G.; Liu, F. Computational design of carbon nanotube electromechanical pressure sensors. *Phys. Rev. B* **2004**, *69,* 153406.

[5] Liu, F. *In situ* pressure monitor and associated methods. Patent, Pub. No. WO/2008/127797, Oct. 23,2008; International Application No. PCT/US2008/055525, Feb. 29, 2008.

[6] Pantarotto, D.; Briand, J. -P.; Prato, M.; Bianco, A. Translocation of bioactive peptides across cell membranes by carbon nanotubes. *Chem. Commun.* **2004**, *1,* 16–17.

[7] Cai, D.; Mataraza, J. M.; Qin, Z. -H.; Huang, Z.; Huang, J.; Chiles, T. C.; Carnahan, D.; Kempa, K.; Ren, Z. Highly efficient molecular delivery into mammalian cells using carbon nanotube spearing. *Nat. Methods* **2005**, *2,* 449–454.

[8] Smith, B. W.; Monthioux, M.; Luzzi, D. E. Encapsulated C-60 in carbon nanotubes. *Nature* **1998**, *396,* 323–324.

[9] Hummer, G.; Rasalah, J. C.; Noworyta, J. P. Water conduction through the hydrophobic channel of a carbon nanotube. *Nature* **2001**, *414,* 188–190.

[10] Gao, H.; Kong, Y.; Cui, D.; Ozkan, C. S. Spontaneous insertion of DNA oligonucleotides into carbon nanotubes. *Nano. Lett.* **2003**, *3,* 471–473.

[11] Longhurst, M. J.; Quirke, N. Temperature-driven pumping of fluid through single-walled carbon nanotubes. *Nano. Lett.* **2007**, *7,* 3324–3328.

[12] Dai, Y.; Tang, C.; Guo, W. Simulation studies of a "nanogun" based on carbon nanotubes. *Nano Res.*

2008, *1,* 176.

[13] Král, P.; Tománek, D. Laser-driven atomic pump. *Phys. Rev. Lett.* **1999**, *82,* 5373–5376.

[14] Insepov, Z.; Wolf, D.; Hassanein, A. Nanopumping using carbon nanotubes. *Nano. Lett.* **2006**, *6,* 1893.

[15] Wang, Q. Atomic transportation via carbon nanotubes. *Nano. Lett.* **2009**, *9,* 245–249.

[16] Ulbricht, H.; Moos, G.; Hertel, T. Interaction of C_{60} with carbon nanotubes and graphite. *Phys. Rev. Lett.* **2003**, *90,* 095501.

[17] Chang, T. Dominoes in carbon nanotubes. *Phys. Rev. Lett.* **2008**, *101,* 175501.

[18] Chopra, N. G.; Benedict, L. X.; Crespi, V. H.; Cohen, M. L.; Louie, S. G.; Zettl, A. Fully collapsed carbon nanotubes. *Nature* **1995**, *377,* 135–138.

[19] Chen, M.; Zang, J.; Xiao, D. Q.; Liu, F. Mechanical wave propagation in carbon nanotubes driven by an oscillating tip actuator. *J. Appl. Phys.* **2009**, *105,* 026102.

[20] Okada, S.; Saito, S.; Oshiyama, A. Energetics and electronic structures of encapsulated C-60 in a carbon nanotube. *Phys. Rev. Lett.* **2001**, *86,* 3835–3838.

[21] Tersoff, J. Sample-dependent resolution in scanning tunneling microscopy. *Phys. Rev. B* **1989**, *39,* 1052–1057.

[22] Rappé, A. K.; Casewit, C. J.; Colwell, K. S.; Goddard III, W. A.; Skiff, W. M. UFF, a full periodic-table force-field for molecular mechanics and molecular-dynamics simulations. *J. Am. Chem. Soc.* **1992**, *114,* 10024–10035.